GREEN SYNTHESIS OF LOW DIMENSINAL MATERIALS FOR THE ADVANCED TECHNOLOGIES

SUMMARY

THESIS SUBMITTED FOR THE AWARD OF THE DEGREE OF

Doctor of Philosophy

In
Applied Physics

By
Surya Pratap Goutam
Enrolment No.: 587/11

Under the Supervision of
Dr. Anil Kumar Yadav

Department of Applied Physics
School for Physical Sciences
Babasaheb Bhimrao Ambedkar University, Lucknow,
U.P., (India) – 226025

2018

GREEN SYNTHESIS OF LOW DIMENSIONAL MATERIALS FOR THE ADVANCED TECHNOLOGIES

This work has been motivated by the outstanding requirement to prepare nanomaterials through a suitable synthesis technique which is efficient, cost-effective and does not utilize any toxic materials in the synthesis. The objectives of the present thesis mainly study of green synthesis and characterization of some metal oxide nanoparticles (TiO_2, CuO, ZnO and Fe_2O_3) and their application in wastewater treatment and biomedical applications. The attempt has been made to extract useful information as much possible from our investigations. The entire thesis work is divided into seven chapters and a summary corresponding to each chapter is given underneath.

Metal oxide nanoparticles have received extensive interest in the recent decades owing to their unique physical and chemical properties which are expected to open new avenues in many technological areas, such as in water treatment, catalysts, semiconductors, energy storage and sensing, targeted drug delivery, antimicrobial application, cancer diagnosis and personal care products etc. [1]. Currently, the development of persistent methods of synthesis of metal nanoparticles for controlling their sizes, shapes and chemical composition is a rapidly growing area of research in the field of Material science. Metal nanoparticles of different sizes, shapes, and compositions can be synthesized by a number of chemicals, physical methods and hybrid methods, which includes laser pyrolysis, sol-gel, plasma spraying process, aerosol-based prosses, chemical vapour deposition, microwave, electrochemical, chemical reduction, photochemical reduction, UV irradiation, lithography etc. [2,3]. Although, these conventional methods are more

popular for the synthesis of metal nanoparticles with the desired size and shape for specific applications. At the same time, they are bound with various limitations such as expense and harmful starting materials, requirement of expensive equipments, generation of hazardous chemicals, the requirement of high temperature and pressure etc. Due to these drawbacks of conventional methods, researchers and scientist are focusing on the novel procedures using biological systems. Various studies show that green synthesis is the rapid, cost-effective and environment-friendly route of synthesis, because it eradicate or abate pollution from the fabrication of the nanomaterials [4]. Green synthesis involves organisms like a plant, bacteria, fungi etc., for the synthesis of nanomaterials. The advantage of using plants and leaf extracts over other eco-friendly biologically systems such as bacteria and fungi, is that it circumvents the use of well-conditioned culture preparation and segregation techniques that are extremely expensive and intricate [5].

For the biosynthesis of metal nanoparticles, plant extract can be prepared from leaves, stems, flower, seeds of various plants. The extract contains biomolecules such as protein, amino acid, enzymes, vitamins, terpenoids, flavonoids, alkaloids, phenolic acids, etc [6]., act as capping and reducing agents that can reduce metal ions during the bioreduction process to produce nanoparticles or nanostructures with different shapes and sizes. These nanoparticles can be used for the applications of electronics, water/wastewater treatment, cancer therapy, sensing, antimicrobial activity and cosmetics. Typical examples are delineated here to summarize the overall potential of green synthesized nanoparticles in environmental and biomedical applications.

Table 1: Illustrating the application of green synthesized nanoparticles in environmental and biomedical applications

Sr. No.	Nanoparticles	Biological materials	Biological agents	Characteristics	Application in dye removal and water and wastewater treatment	Ref.
1.	α-Fe_2O_3 NPs	Plant leaf extract	*Curcuma* and *Tea*	Crystallite size: using Curcuma (4 nm); using Tea (5 nm); Shape: spherical	Degradation of methylene orange	[7]
2.	Cuprous oxide (Cu_2O)	Plant leaf extract	*Calotropis gigantean*	Size: 8.8 nm; Shape: Octahedral, dodecahedra, and cubic	90 % MB dye removal after light exposure 120 minutes	[8]
3.	Au NPs	Plant leaf extract	*Lagerstroemia speciosa*	Size: 41 - 91 nm; Shape: hexagonal	Photocatalytic reduction of organic pollutants (methylene blue (MB), methyl orange (MO), bromophenol blue (BPB), and bromocresol green (BCG) dyes and nitro aromatic compound (4-nitrophenol (4-NP); Photocatalytic reduction of dyes with a reduction efficiency of ≥ 90%.	[9]
4.	Silver (Ag) NPs	Plant leaf extract	*Ocimumgratissim um*	Size:16 ± 2 nm; Shape: Triangular	Synthesized NPs were shown higher effective antibacterial activity against E. Coli	[10]
5.	ZnO NPs	Lemon juice	Lemon fruits	Size: ~ 21.5 nm; Shape:	Photocatalytic degradation of	[11]

				spherical	dyes (methyl orange, methyl red and methylene blue)	
6.	Fe NPs	Plants leaf extracts	*Azadiracta indica* (AI), *Magnolia champaca*(MC), *Mangifera indica* (MI) and *MurrayaKoenigii*(MK)	Size: (AI: 96 - 110 nm); (MC :99 - 129 nm); (MI and MK :100 - 150 nm); Shape: spherical	Treatment of domestic wastewater; AI-Fe NPs showed maximum removal efficiency (phosphates removal: 98.1%; ammonium nitrogen removal: 84.3%; and COD removal: 82.4%)	[12]
7.	Zinc Oxide (ZnO) NPs	Flower extract	*Trifoliumparatense*	Size: 60-70 nm	Synthesized NPs were shown high activity against S.aureous ATCC 4163, E. Coli ATCC 25922, P. aeruginosa 6749, S. aureous and P. aeruginosa.	[13]
8.	Iron oxide NPs	Peel extract	*Tangerine*	Size: ~ 50 nm; Shape: spherical	Treatment of contaminated solution (Cd removal: 90%)	[14]
9.	Fe_3O_4	Seaweeds (Algae)	*Padinapavonica (PP)* and *Sargassumacinarium (SA)*	Size: PP (10 - 19.5 nm) and SA (21.6 - 27.4 nm); Shape: spherical	Bioremoval of Pb removal using PP: 91%, Pb removal using SA: 78%	[15]
10.	ZnO NPs	Plant leaf extract	*Plectranthus amboinicus*	Average size: 88 nm; Shape: rod shape	Degradation of methyl red (MR)	[16]
11.	FeO NPs	Plant leaf extract	*Amaranthus spinosus*	Maximum particle size: 91 nm; Shape: spherical	Decolourization of dyes (methyl orange: 75% and methylene blue: 69%)	[17]
12.	Nano zero-valent iron (nZVI)	Tea extract	*Camellia sinensis*	Size: 5 - 15 nm; Shape: spherical	Degradation of bromothymol blue	[18]
13.	Potassium Zinc Hexacyanoferr	Natural surfactant	*Sapindusmukorossi*	Size: 33 - 192 nm; Shape: cubic	Photocatalytic degradation of organic dyes	[19]

	ate Nanocubes				(Malachite Green (MG): 94.15% and Eriochrome Black T (EBT): 76.13%)	
14.	Fe NPs	Tea extract	Green Tea (GT), Oolong Tea (OT), and Black Tea (BT)	Size: GT-FeNPs (20 - 40 nm), Shape: irregular spherical	Treatment of wastewaters by removal of monochlorobenzene (MCB) (MCB removal using GT: 69%, MCB removal using OT: 53%, and MCB removal using BT: 39%)	[20]
15.	Ag NPs	Plant leaf extract	*Zanthoxylumarmatum*	Size: 15 - 50 nm; Shape: spherical	Degradation of dyes (degradation rate constant value of Safranine O: 1.02×10^{-3} Min^{-1}; degradation rate constant value of Methyl red: 1.03×10^{-3} Min^{-1}; degradation rate constant value of Methyl orange: 1.86×10^{-3} Min^{-1}; 10.degradation rate constant value of Methylene blue: 1.44×10^{-3} Min^{-1}	[21]
16.	Fe NPs	Plant extracts and juices	Extracts of *Camellia sinensis* (green tea, GT), *Syzygiumaromaticum* (clove, CL), *Menthaspicata* (spearmint, SM), *Punicagranatum* juice (pomegranate, PG) and Red Wine (RW)	Sizes: 50 - 60 nm; Shape: spherical	Reduction of hexavalent Cr	[22]
17.	Copper oxide (CuO) NPs	Gum	*Gum karaya*	Size: 4.8±1.6 nm; Shape: Spherical	Smaller size of synthesized NPs were shown	[23]

					higher antibacterial activity against E. Coli and S. aureous	
18.	Copper oxide (CuO) NPs	Plant leaf extract	*pomegranate*	Size: 40-78 nm; Shape: Spherical	Impregnated carbons with CuO NPs were shown great removal of water pollutants mainly nitrate	[24]
19.	Ag NPs	Plant leaf extract	*Focus Benjamina*	Size: 60 - 105 nm	Maximum Cd removal from aqueous solution: 85%	[25]
20.	Ag NPs	Plant leaf extract	*Piliostigma thonningii*	Size: 50 - 114 nm; Shape: spherical	Heavy metal removal activity (max. iron ion removal: 96.9%; max. copper removal: 89%; max. lead removal: 97.89%; max. magnesium removal: 93.6%)	[26]
21.	Cu NPs	Peel extract	*Citrus grandis*	Size: 22-27 nm; Shape: spherical	Degradation of methyl Red: 96%	[27]
22.	Ag-NPs	Petals extract	*Rosa* 'Andeli'	Size: 4 - 29 nm; Shape: spherical	Degradation of commercial dye Putnam sky blue 39 with an efficiency of 95%	[28]
23.	ZnO, CuO, Co_3O_4, NiO and Cr_2O_3	-	Sunlight Irradiation	Size: ZnO; <35 nm; CuO; 7 - 50 nm; Co_3O_4; 45-90 nm; NiO; 2 - 25 nm; Cr_2O_3: ~ 17 nm; Shape: ZnO (nanotubes); CuO (nanorods); Co_3O_4 (triangles and hexagons); NiO(needle-shaped) and Cr_2O_3	Treatment of simulated water containing hazardous dyes: removal dyes mixture (Alizarin Red S (ARS) + Methylene Blue (MB) (removal using Cr_2O_3: 88.24%; removal using > removal using ZnO: 87.96% > removal using CuO:	[29]

				(nanobeads)	86.86% > removal usingNiO: 85.89% > removal using Co_3O_4: 80.35%	
24.	Fe NPs	Plant leaf extracts	*Eucalyptus* sp.	Size: 20 - 80 nm; Shape: spheroidal	Treatment of eutrophic wastewater (N removal: 71.7%; P removal: 30.4%; and COD removal 84.5%)	[30]
25.	Iron NPs	Tea extract	*Tie Guanyin*	Size: 6.58 ± 0.76 nm; Shape: spherical	Degradation of dye (Bromothymol Blue removal: more than 90%)	[31]
26.	Au and Ag NPs	Plant stem extract	*Breyniarhamnoides*	Au: ~ 25 nm; Ag: ~ 64 nm; shape: spherical	Catalytic conversion of 4-nitrophenol (4-NP) to 4-aminophenol (4-AP)	[32]
27.	AgNPs-Soil nanocomposite	Plant leaf extract	*Ocimumtenuiflorum*	Size: 20 - 40 nm; Average Size: 32.58 nm	Treatment of textile dye (turquoise blue dye removal: 96.8%)	[33]
28.	Reduced Graphene Oxide (RGO)/Fe_3O_4 Nanocomposites	Plant leaf extract	*Solanumtrilobatum*	Size:18 nm; Shape: spherical	Degradation of methylene blue: 95.9%	[34]
29.	Fe NPs	Plant leaf extracts	Green tea (*Camellia sinensis*) and Pomegranate (*Punicagranatum*)	-	95% color removal and almost 80% dissolved organic carbon removal From Textile Wastewater	[35]

Chapter 2: Experimental Techniques

This chapter gives details of characterization techniques employed for the analysis of synthesized metal oxide nanoparticles. These include Scanning electron microscopy, Field emission scanning electron microscope, Transmission electron microscopy, Energy dispersive X-Ray spectroscopy, X-Ray powder diffraction, Ultraviolet-Visible spectroscopy, Fourier transform infrared spectroscopy and Dynamic light scattering, Brunauer-Emmett-Teller (BET) and Barret-Joyner-Halenda (BJH), Inverted microscope, Photoluminescence spectrophotometer etc.

Chapter 3: Green synthesis of TiO_2 nanoparticles using leaf extracts of *Jatropha curcas L.* for photocatalytic degradation of tannery wastewater

This chapter is aimed at the synthesis of titanium dioxide (TiO_2) NPs and evaluates its performance for the photocatalytic treatment of TWW after the secondary (biological) treatment process. *Herein,* biodiesel plant, *Jatropha curcas L.* leaves were used for the green synthesis of TiO_2 NPs. Firstly, fresh leaves were washed thoroughly with DD water to remove the associated dust particles and cut it into the fine pieces and then dried in the presence of for the preparation of leaf extracts. For the synthesis of TiO_2 NPs, 80 ml of 0.50 M $TiCl_4$ was added to the 80 ml of filtered leaf extracts in a ratio of 1:1 (v/v) with a continuous stirring at room temperature. After precipitation of NPs were separated out from the solution through filtration, followed by washing with ethyl alcohol to remove the ionic impurities. Afterward, the washed precipitates were air dried and calcined at 450 °C for 3 h in a muffle furnace and then finely grind in a crystal mortar pestle to obtain the final powder form of TiO_2 NPs. Now, morpho- structural characterization of green synthesized TiO_2 NPs were done by XRD, SEM etc. The Results confirmed the

synthesis and anatase phase of the spherical TiO_2 NPs and also unfold the presence of phytochemicals in leaf extract, which might involve in the capping/stabilization of NPs.

Photocatalytic treatment of secondary treated tannery wastewater

The solar photocatalytic activity of the green synthesized TiO_2 NPs were performed using self-designed parabolic trough reactor photocatalytic treatment to testify its potential for the simultaneous removal of chemical oxygen demand (COD) and chromium (Cr) from secondary treated tannery wastewater. During the photocatalytic treatment of wastewater in a self-designed and fabricated Parabolic Trough Reactor (PTR), 82.26% removal of COD and 76.48% removal of Cr from TWW were achieved. The higher solar photocatalytic activity of the green synthesized TiO_2 NPs can be attributed to the nano-size, pure crystalline anatase phase, large amount surface hydroxyl groups and higher surface area. Overall, the green synthesized TiO_2 NPs demonstrated the astounding potential for the in situ treatment of TWW as an alternative clean-green treatment solution.

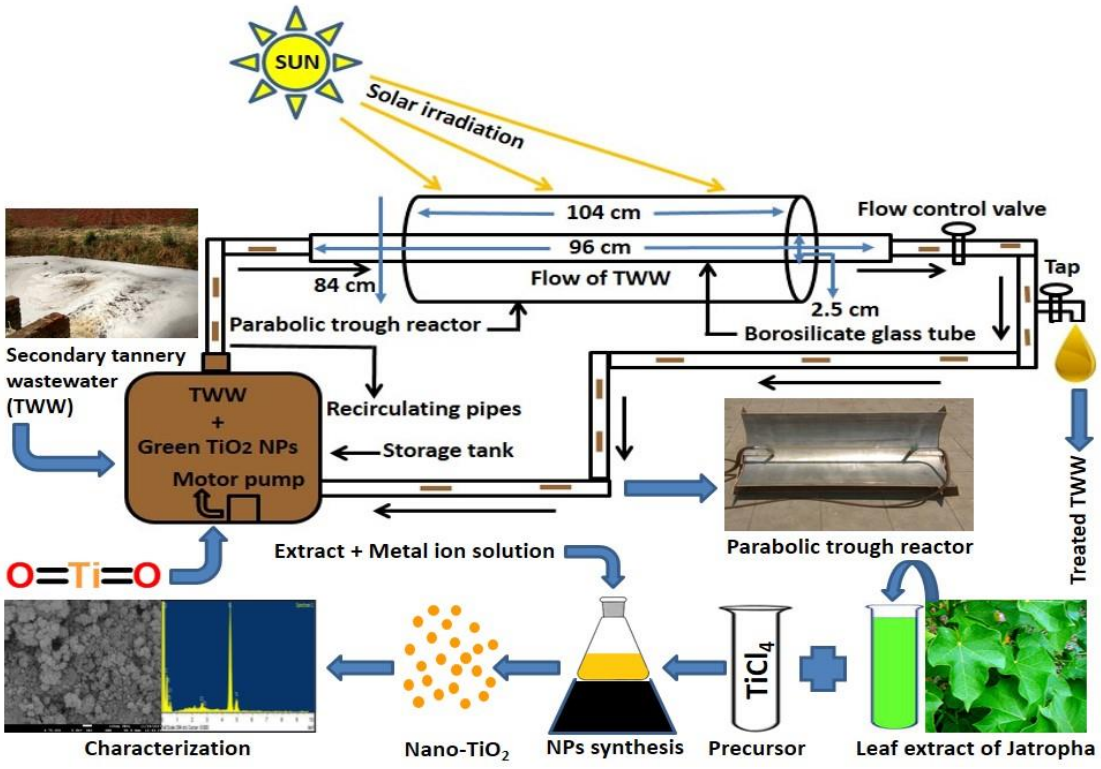

Fig. 1: Graphical representation of synthesis, characterization and application of TiO_2 NPs.

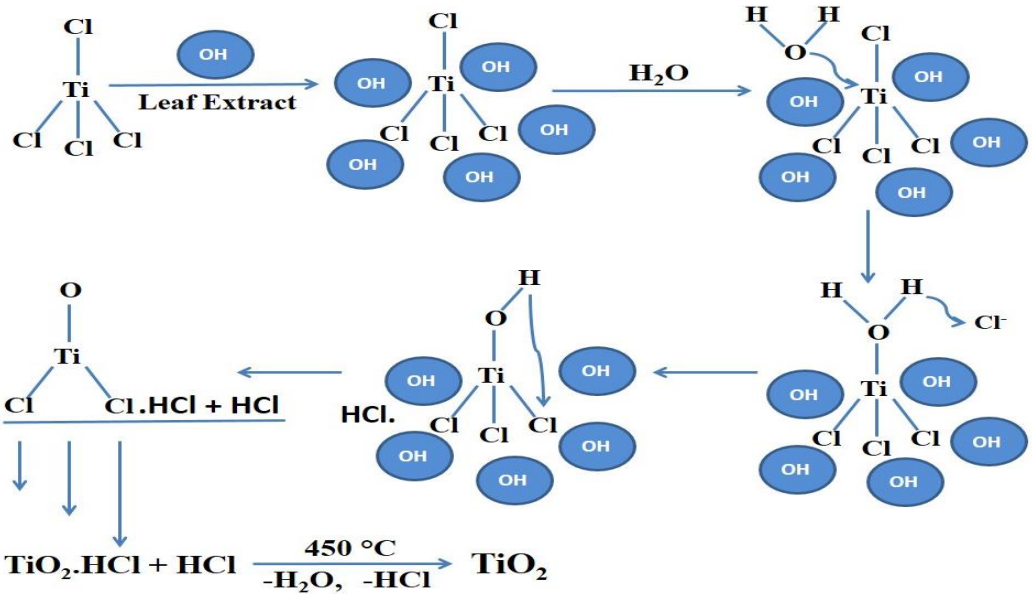

Fig. 2: Possible reaction mechanism for the formation of TiO_2 NPs in presence of hydroxyl group (-OH) of leaf extract of *Jatropha curcas* L. as capping agent.

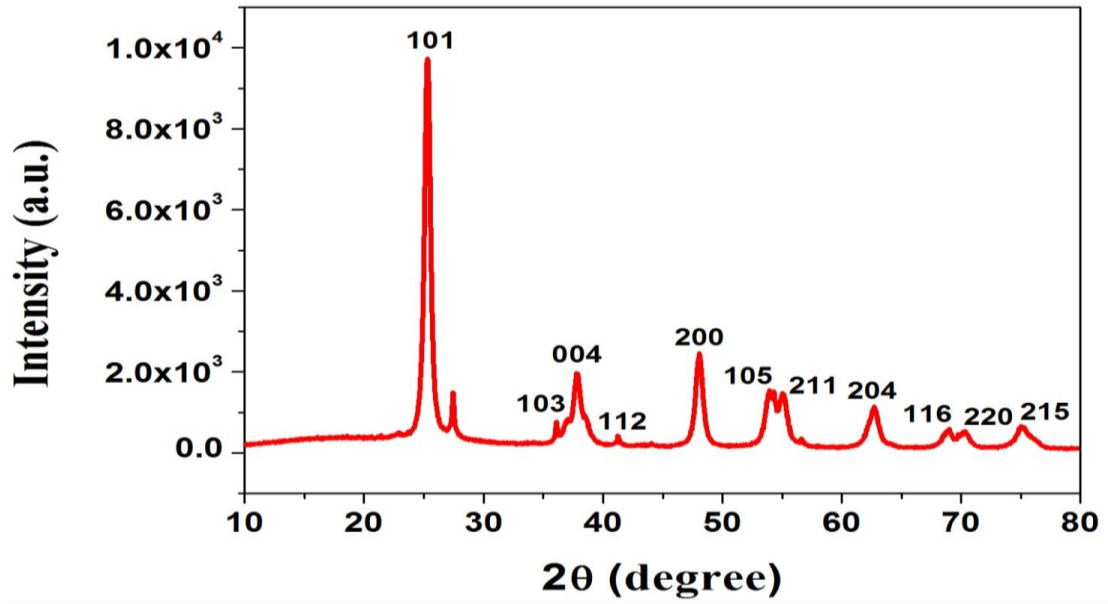

Fig. 3: X-Ray diffraction pattern of green synthesized anatase TiO_2 NPs.

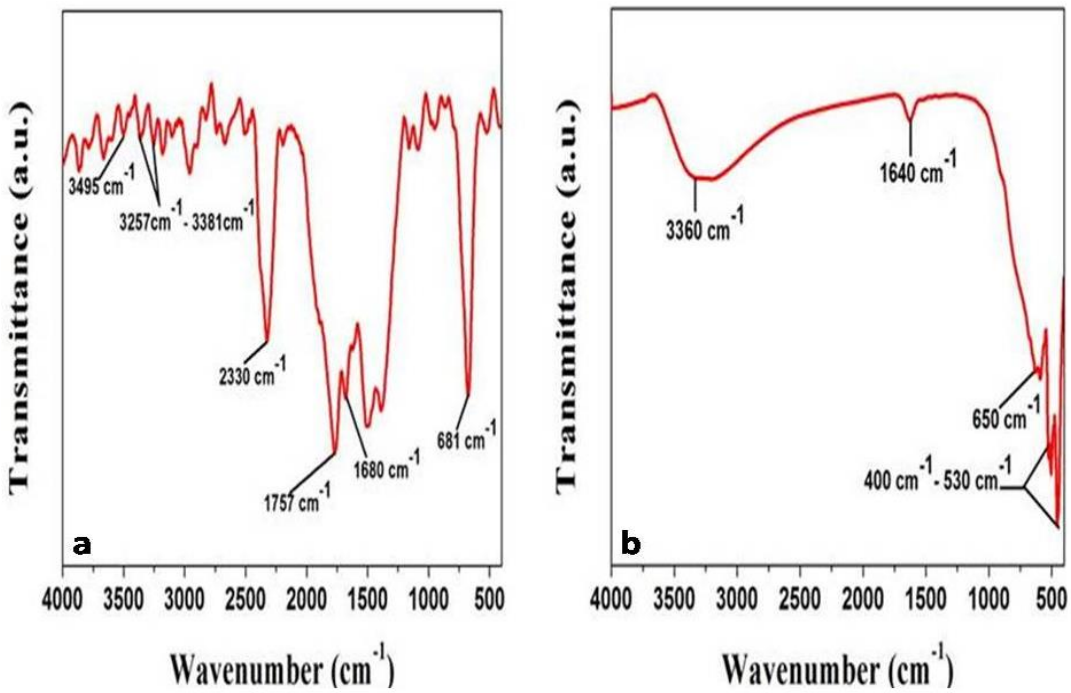

Fig. 4: (a) FT-IR spectra of leaf extracts of *Jactropha curcus* L. (b) green synthesized TiO_2 NPs.

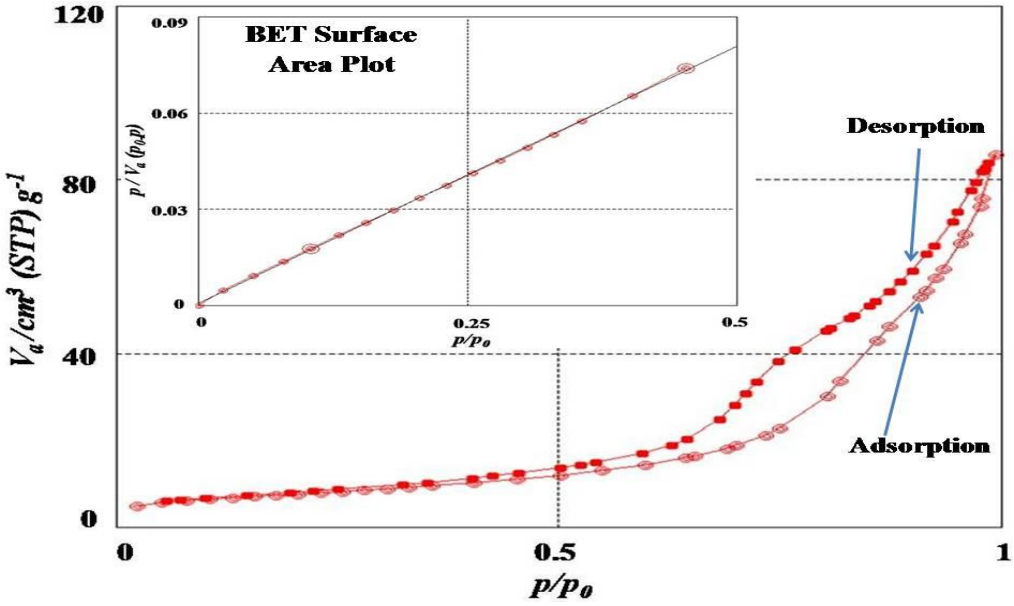

Fig. 5: (a) N_2 Adsorption/desorption isotherm of the green synthesized TiO_2 NPs.

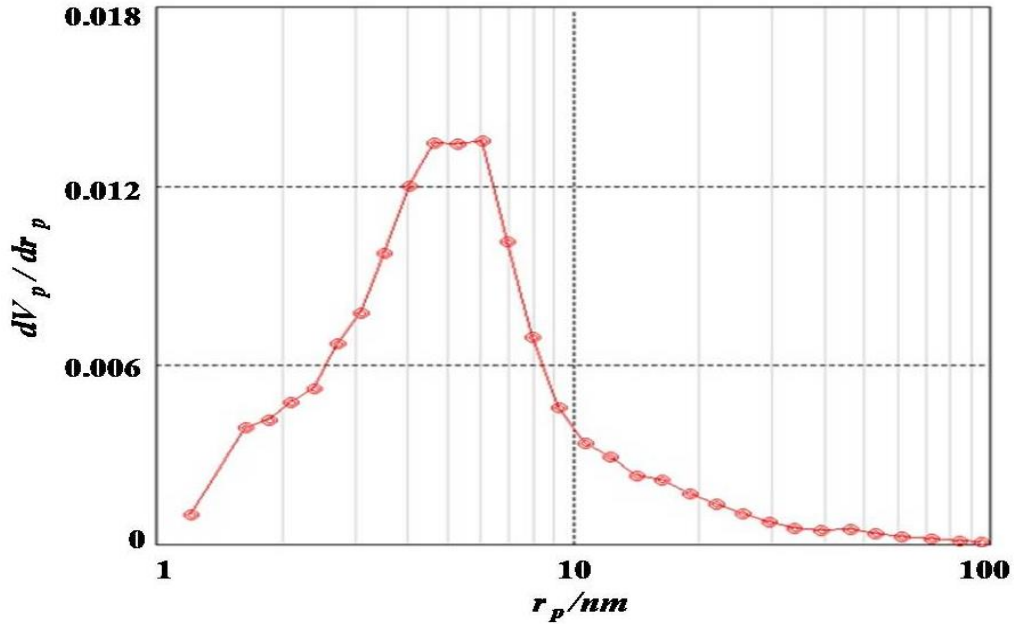

Fig. 5 (b) BJH plot of the green synthesized TiO_2 photocatalyst

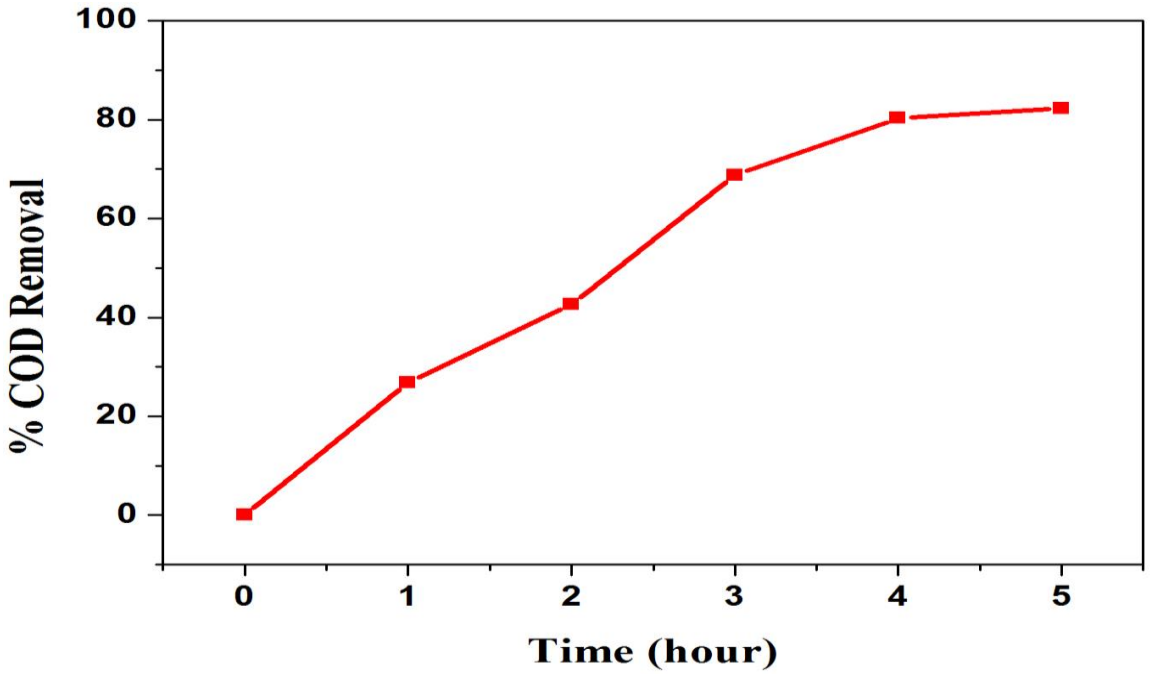

Fig. 6: COD degradation profile during solar photocatalytic treatment of TWW with green synthesized TiO_2 NPs.

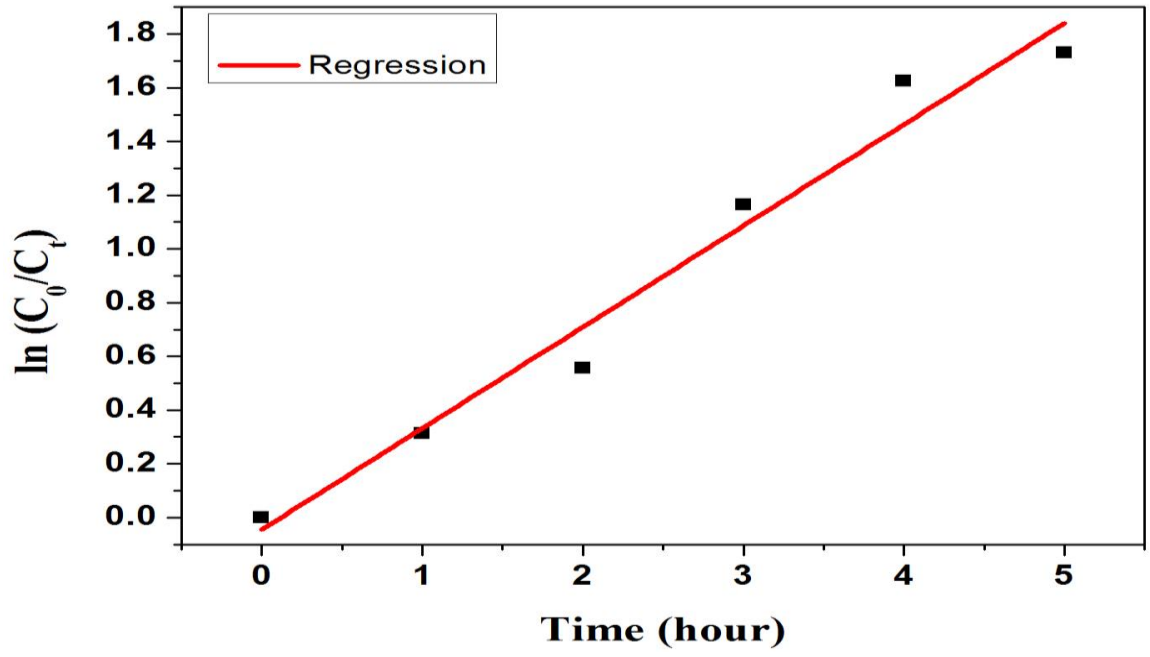

Fig. 7: Kinetic data for COD degradation during solar photocatalytic treatment of TWW with green synthesized TiO_2 NPs.

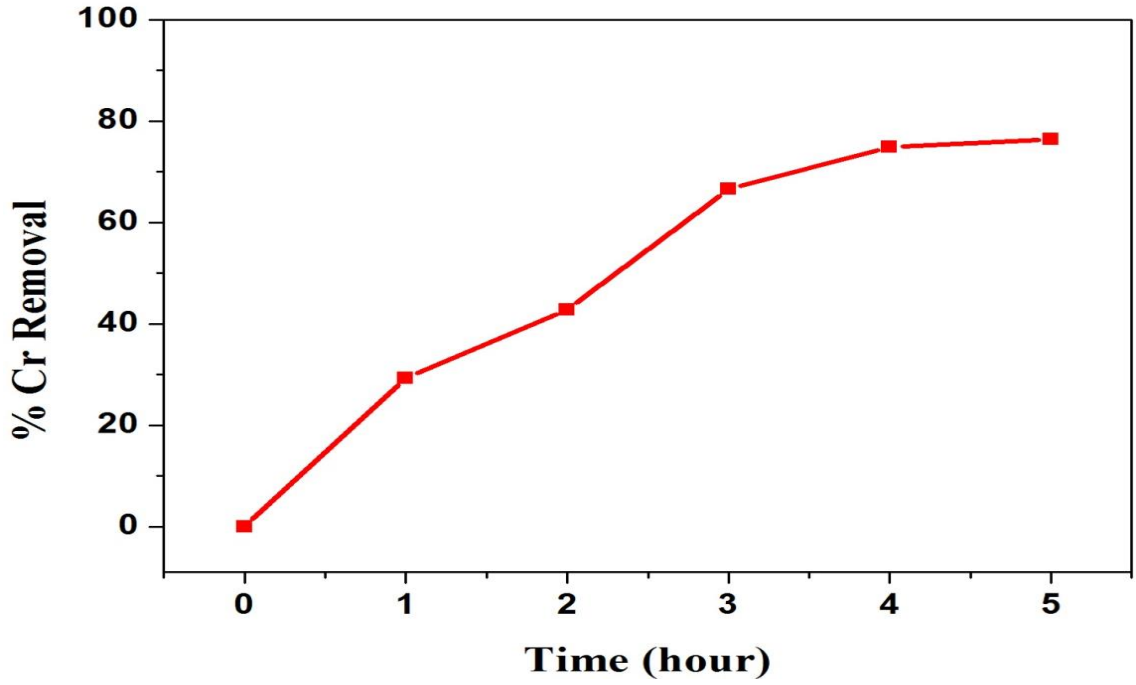

Fig. 8: Cr removal profile during solar photocatalytic treatment of TWW with green synthesized TiO_2 NPs.

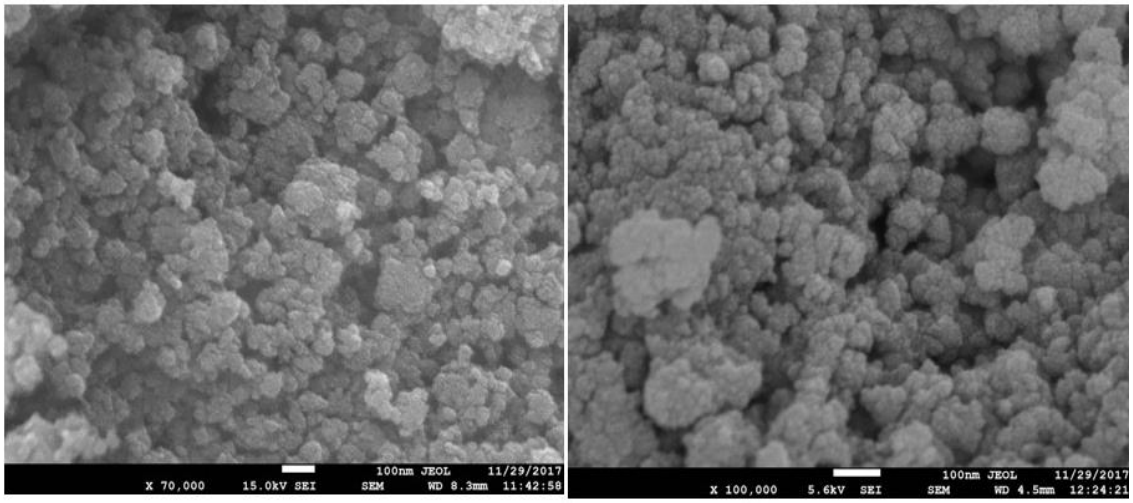

Fig. 9: (a) FESEM images of green synthesized TiO_2 NPs after photocatalytic treatment of TWW.

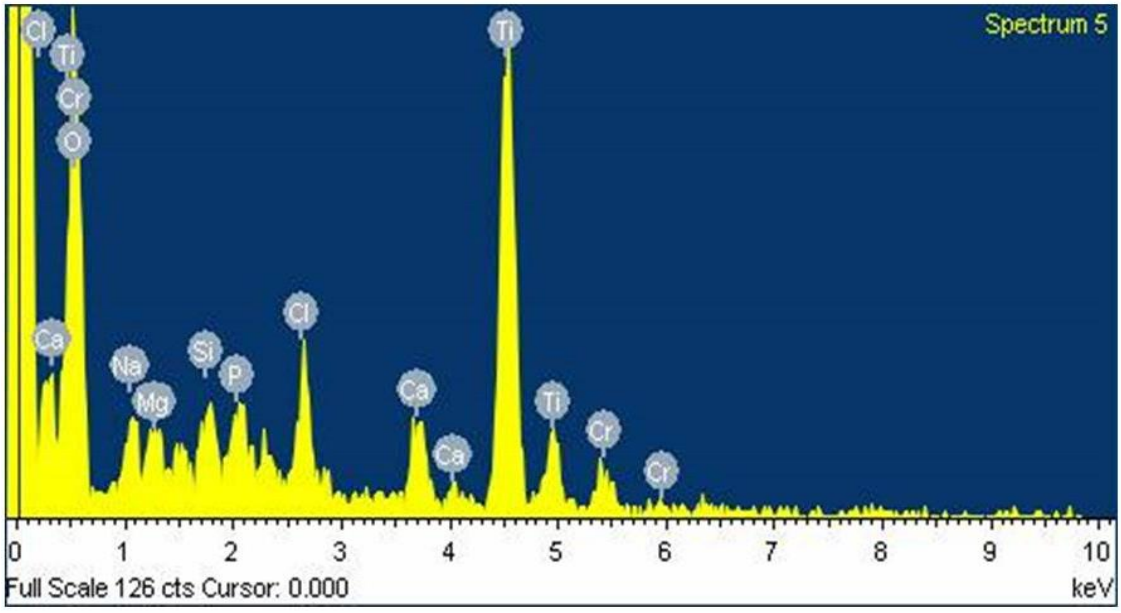

Fig. 9: (b) EDS spectrum of green synthesized TiO_2 NPs after photocatalytic treatment of TWW.

Chapter 4: Green Synthesis of Copper Oxide Nanoparticles Using Leaf Extract of Jatropha Curcas L. for Cytotoxicity Test in Hepatocellular Liver Carcinoma

This study has been focused on the green synthesis of copper oxide nanoparticles using fresh leaf extract of Jatropha curcas L. and performed for cytotoxicity test against hepatocellular carcinoma HepG2 cancer cell. For the green synthesis of CuO NPs, 100 ml of 0.2 M Copper (II) Nitrate ethanolic solution added first to leaf extract in ratio 1:1 with continuous stirring at room temperature. Subsequently, 20 ml of 25% ammonia solution slowly added under stirring for the precipitation. The obtained precipitate was washed, dried for 24 hours and calcined at 800^0C in a furnace; black powder of copper oxide nanoparticles was obtained. Characterization of synthesized material has been done using different techniques such as XRD (X-ray Diffraction), FESEM (Field Emission Scanning Electron Microscopy), UV-VIS and EDS. FESEM images confirm the

existence of spherical copper oxide NPs. We have found the average crystallite size of copper oxide NPs as 45 nm. Leaves extract of Jatropha curcas L. plays a significant role in rapid and large-scale synthesis of nanoparticles Moreover, for the cytotoxicity test of green synthesized CuO NPs in hepatocellular liver carcinoma Cell viability assay was carried out using MTT dye. CuO NPs showed the significant results on the mammalian cell through the killing of cancer cells without any evil effect on hepatocytes. At the higher dose of 20 μM, results in remarkably increase in cytotoxicity which is due to the ability of copper oxide nanoparticles to penetration of cell membrane and finally showed IC_{50} value at 45 μM . This is may be due to the binding of the CuO nanoparticles, produced by green synthesis pathway, with cellular biomolecules. This binding may be disrupt the cellular function of the biomolecules. Therefore, CuO NPs can be successfully applied for the treatment of liver cancer since it has sufficient transport properties and cell membrane penetration power.

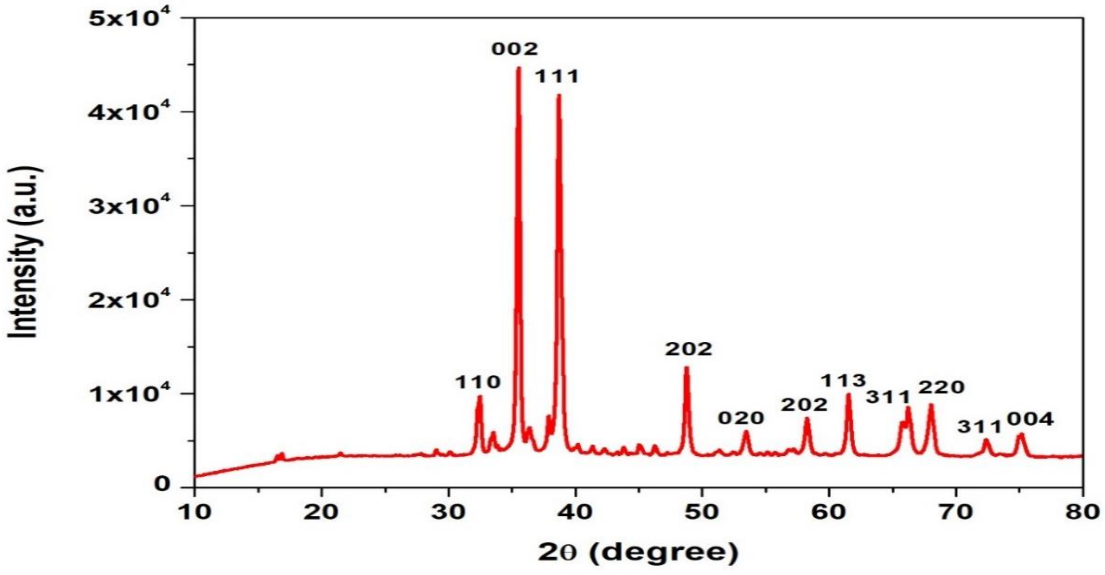

Fig. 10: XRD pattern of copper oxide nanoparticles

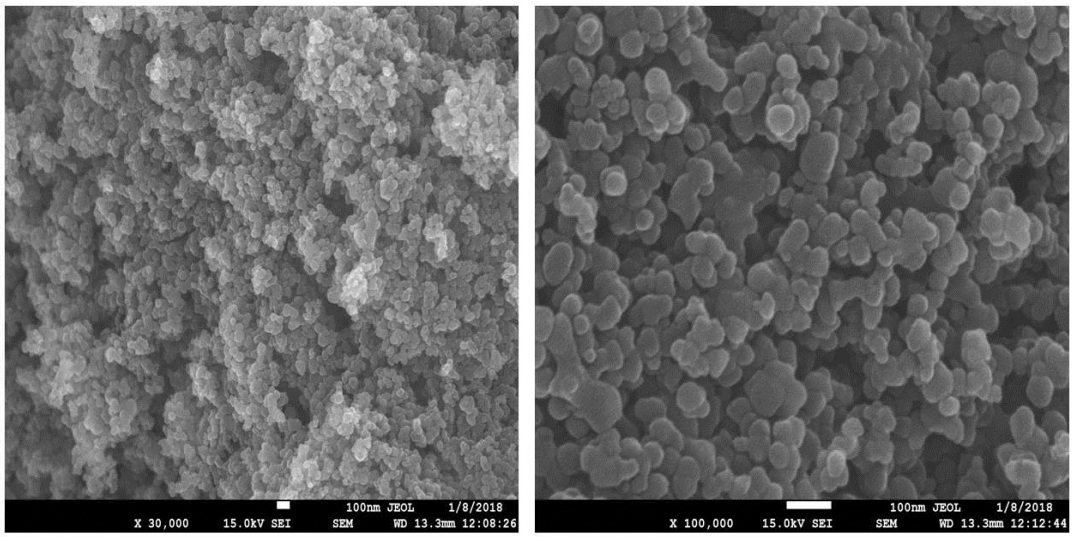

Fig. 11: SEM images of green synthesized copper oxide nanoparticles

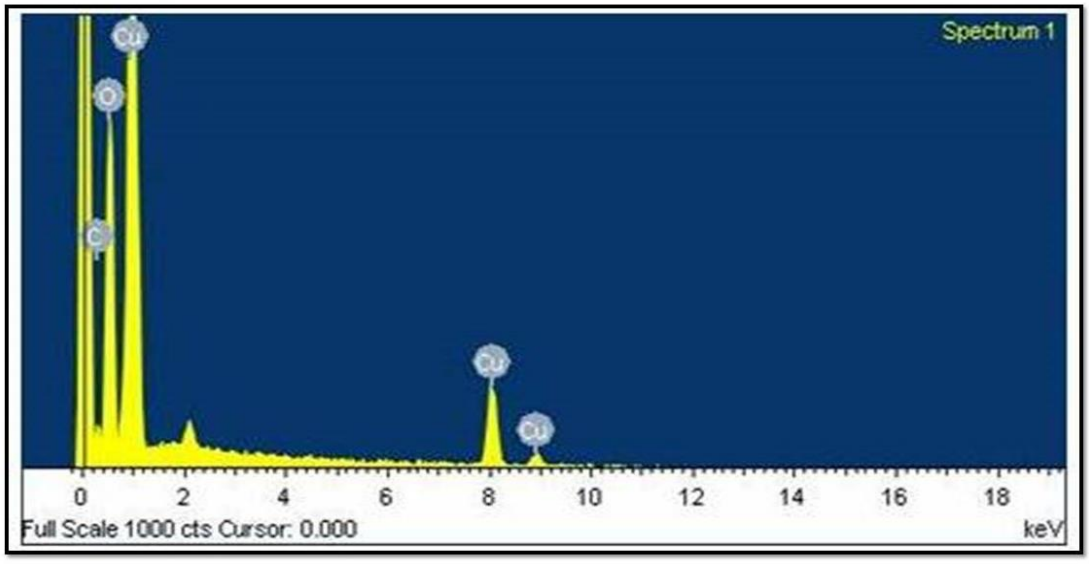

Fig. 12: EDS spectra of green synthesized copper oxide nanoparticles

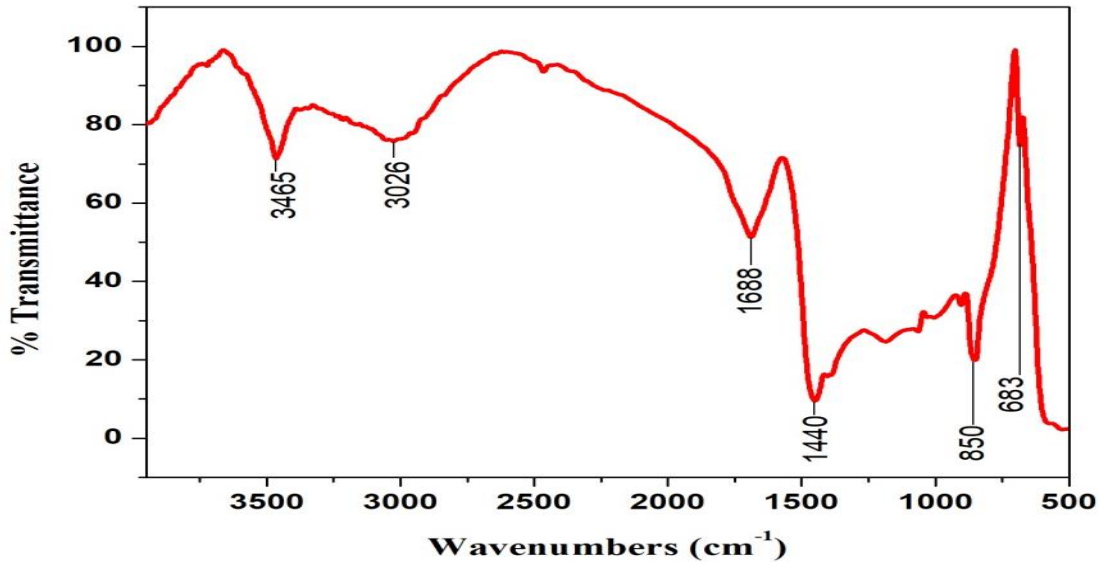

Fig. 13: FTIR spectra green synthesized copper oxide nanoparticles

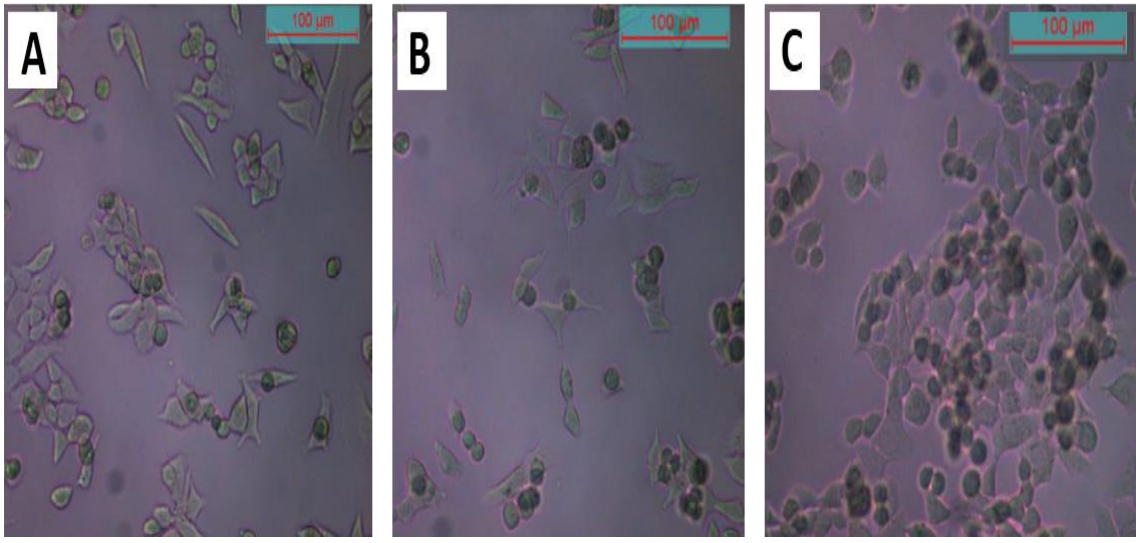

Fig. 14: Cellular morphology of HepG2 cells alone (A), treated for 24 h with10 µM copper oxide nanoparticle (B) and 20 µM copper oxide nanoparticle (C)

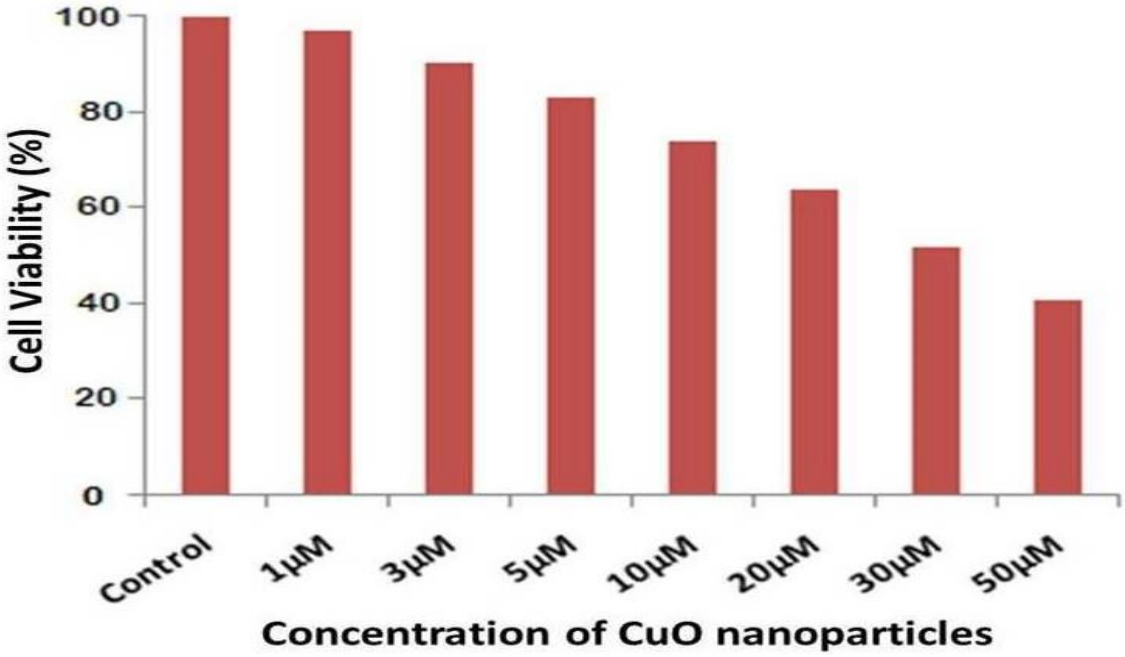

Fig. 15: Effect of copper oxide nanoparticle on HepG2 cell viability at different concentration of copper oxide nanoparticle.

Chapter 5: Coriander Extract Mediated Green Synthesis of Zinc Oxide Nanoparticles and Their Structural, Optical and Antibacterial Properties

In this work, synthesis, morpho-structural characterization, optical and antibacterial properties of zinc oxide nanoparticles have been reported. Zinc oxide nanoparticles were prepared at room temperature via the green route using *Coriandrum sativum* leaf extract. For the green synthesis of ZnO NPs, 100 mL of 0.1 M zinc acetate dihydrate was added first to leaf extract in ratio 1:1 with continuous stirring at room temperature for complete dissolution. Subsequently 20 mL of 1.0 M NaOH solution was slowly added under stirring to increase the pH value and in turn for the precipitation. A progressive change in the color of the solution was observed during the stirring process and the change from sturdy brown to yellowish white confirms the nanoparticles formation.

The product was characterized by a different technique for the structure, morphology and optical properties. Morphology study indicates the spherical nature of the nanoparticles and the formation of zinc oxide nanoparticles was confirmed by EDX. XRD analysis showed the crystalline nature of the ZnO with an average crystallite size of 60 nm which was also corroborated by SEM and TEM analyses. Furthermore, the estimated band gap was 3.8 eV as determined by UV-Visible spectral analysis.

Antimicrobial Activity of Zinc Oxide Nanoparticles

Agar well diffusion method was used to assess the antimicrobial activity of green synthesized zinc oxide nanoparticles. Antibacterial efficacy of the prepared nanoparticles against the pathogenic bacteria E. coli reveals that the ZnO nanoparticles have considerably higher antibacterial potential and is possibly due to a combination of events. The investigation synthesis certainly contributes to growing the knowledge base needed to design suitable antibacterial materials and framework for advanced and wise applications.

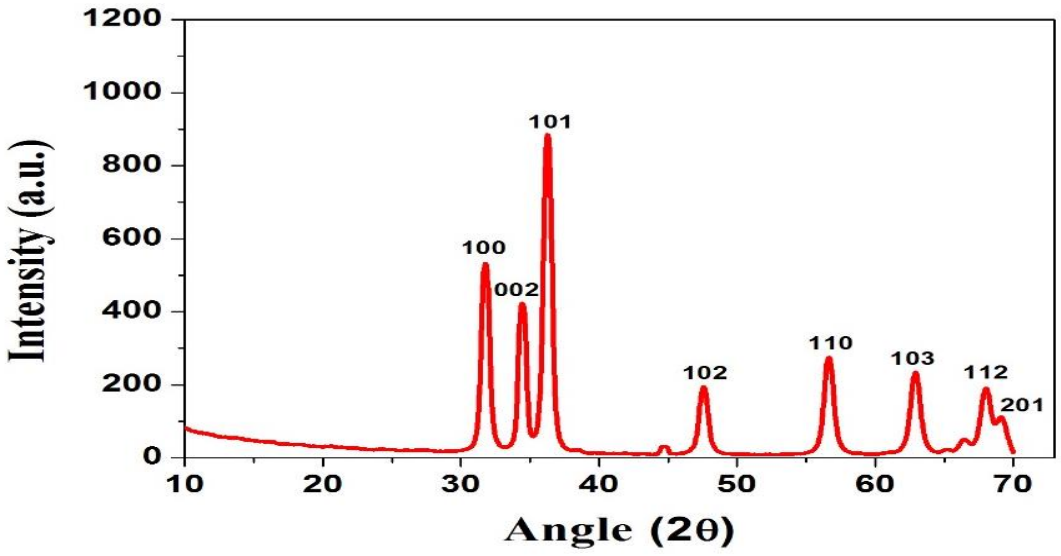

Fig. 16: XRD pattern of Zinc Oxide NPs

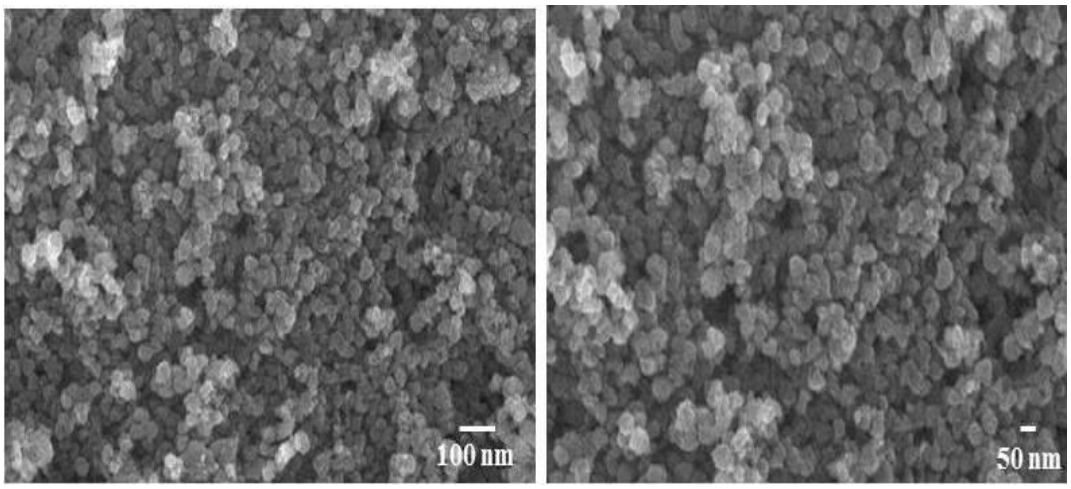

Fig. 17: SEM images of ZnO NPs

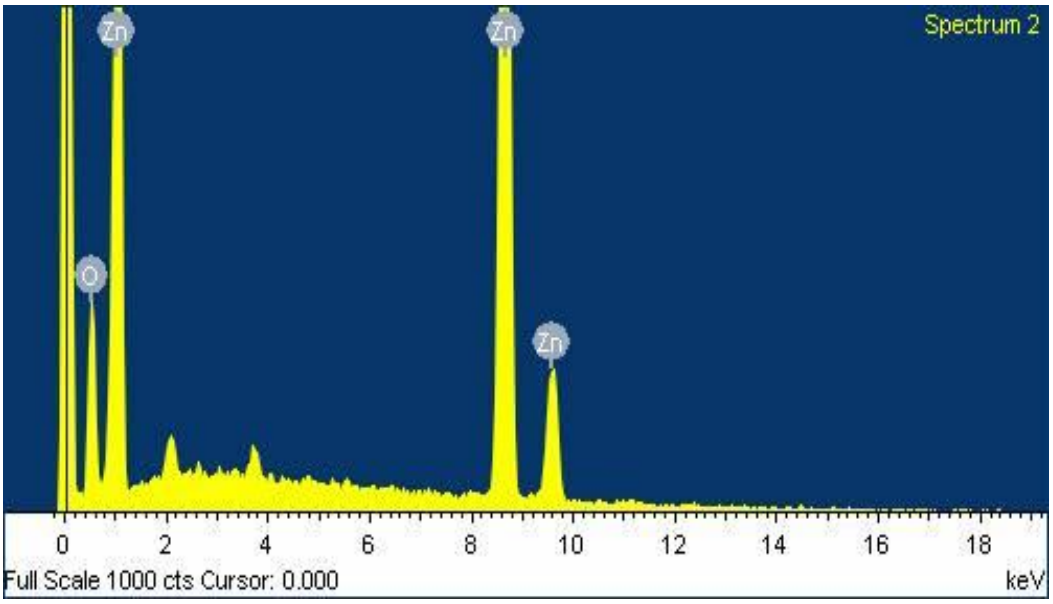

Fig. 18: EDS spectra of aqueous extract of Coriandrum ZnO NPs revealed by green synthesis method

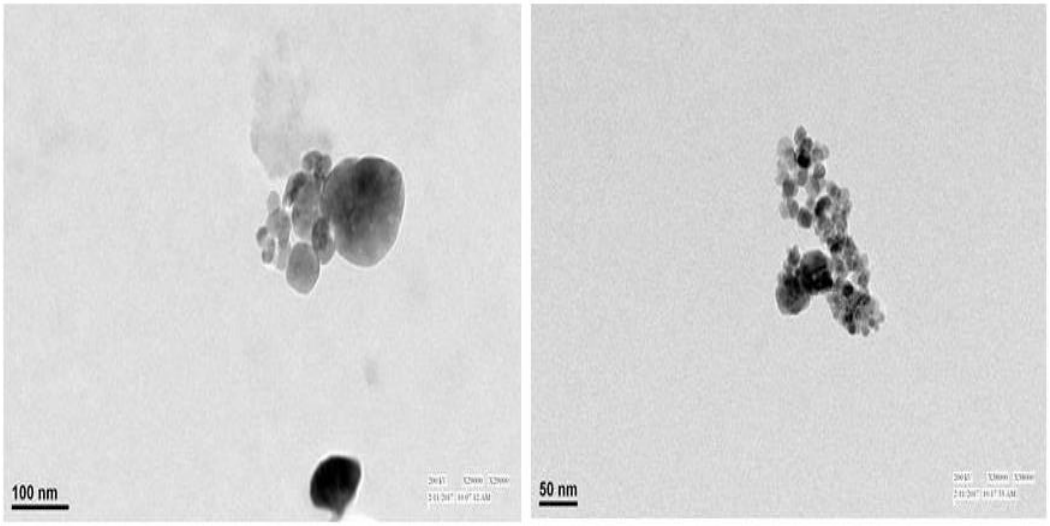

Fig. 19: TEM images of synthesized zinc oxide nanoparticles by Coriandrum leaf

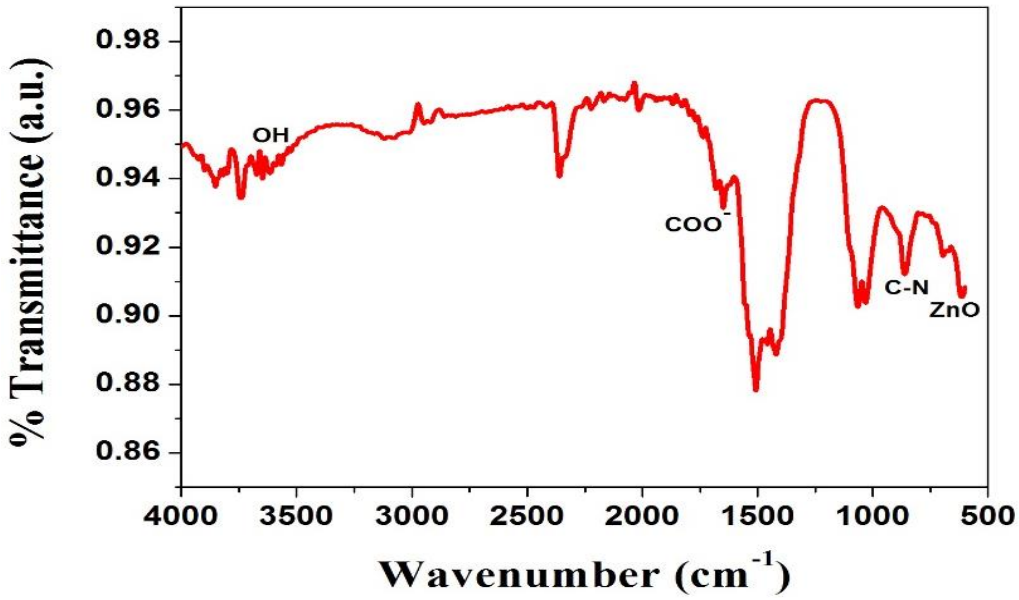

Fig. 20: FTIR of ZnO nanoparticles synthesized using Coriandrum leaf extract

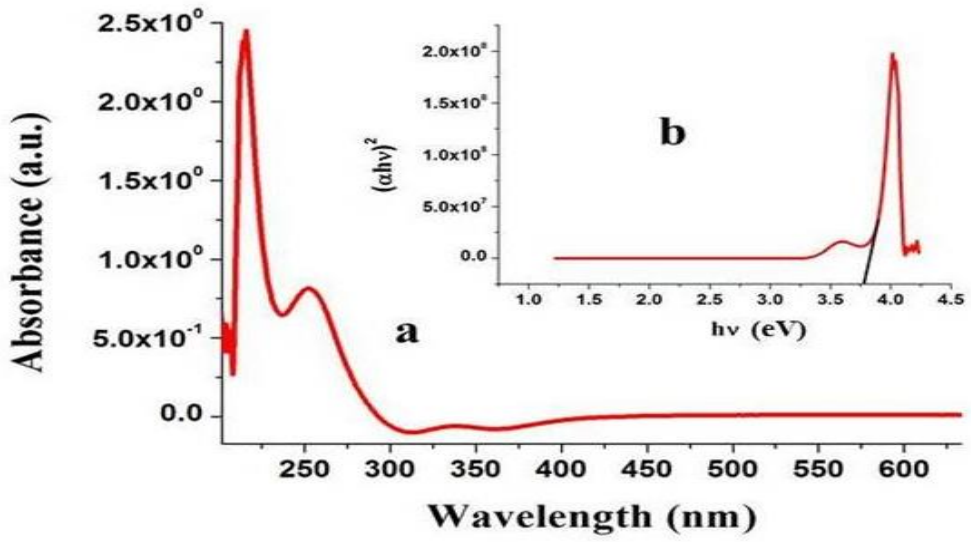

Fig. 21: (a) Absorption spectrum of ZnO nanoparticles **(b)** Tauc plot of ZnO

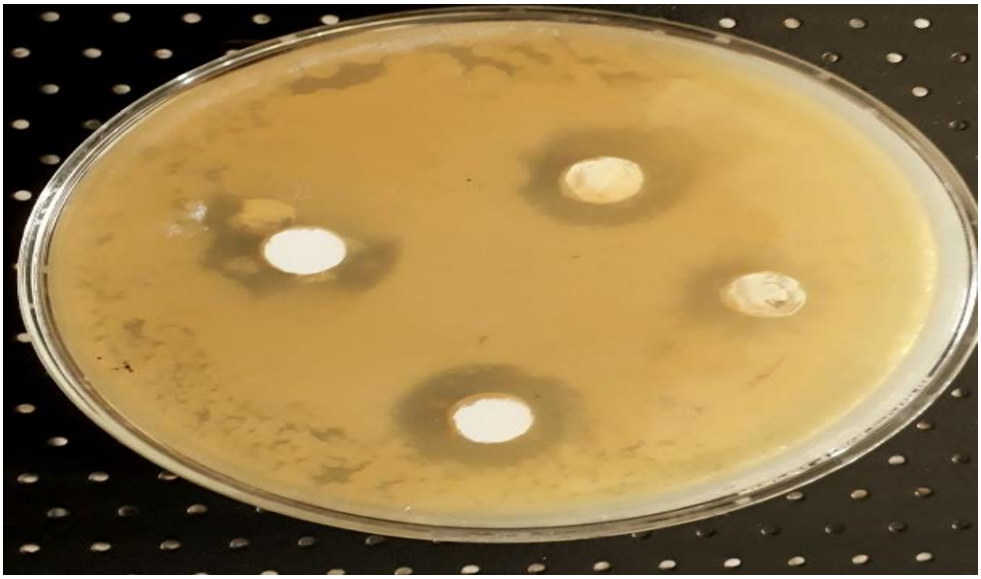

Fig. 22: (a) Antibacterial activity of ZnO NPs having 100 mg/mL, 200 mg/mL, 300 mg/mL and 400 mg/mL concentrations

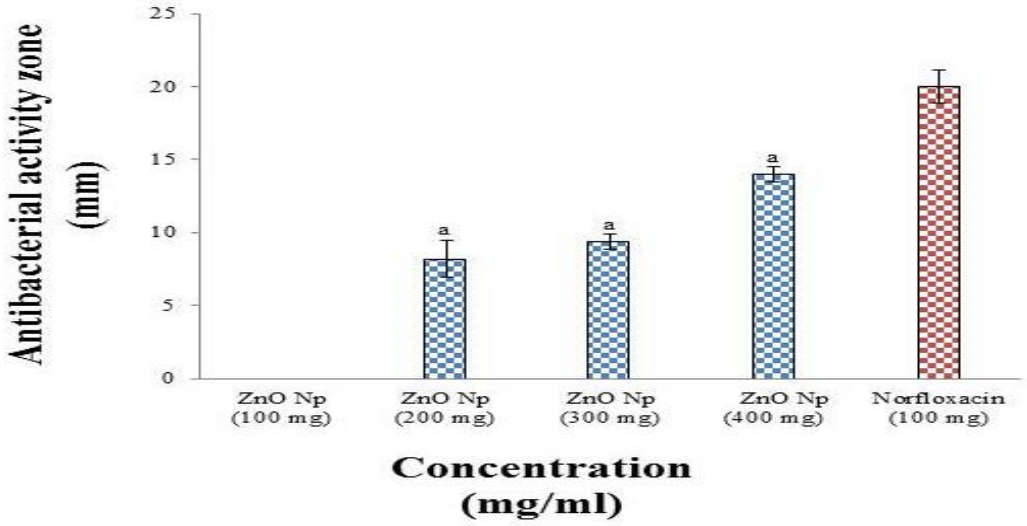

Fig. 22: (b) Antibacterial activity (zone of inhibition, mm) of zinc oxide nanoparticle solution against pathogenic *Escherichia coli.* (ZnO Np = Zinc oxide nanoparticle; Average value given is mean of three replicates with standard deviation and significant value were predicted by using ANOVA (^{a} $p < 0.01$, ^{b} $p < 0.05$) by comparing data of each concentration of ZnO NPs with 100mg Norfloxacin).

Chapter 6

Synthesis of Nanosized Iron Oxide by Leaf Extract of Coriandrum Sativum and its Antimicrobial Properties

The emergence of different types of multi-drug resistant bacterial strains to traditional antibiotics has become a serious concern for the public health [36, 37]. Consequently, for obvious trepidations, it has become vital to explore new and promising antibacterial agents with synergistic properties to abate the actions of such pathogens. To work in this direction, Iron oxide NPs were synthesized by mixing aqueous leaves extract of *Coriandrum sativum* and 0.2 M ferric chloride ($FeCl_3$) solution in the volume ratio 1:1. Adding of 20 ml of 2M NaOH solution to the precursor and leaf extract solution drop-

wise under continuous stirring at room temperature gives a precipitate. Subsequently, the washed precipitate was air dried and annealed at 450 °C for 2 h in a muffle furnace, and then finely ground in a crystal mortar pestle to get the iron oxide NPs in powder form. For the identification of phase and crystallinity, morphology and optical properties of the product was characterized. The average crystallite size of iron oxide NPs from XRD pattern was found to be 80 nm.

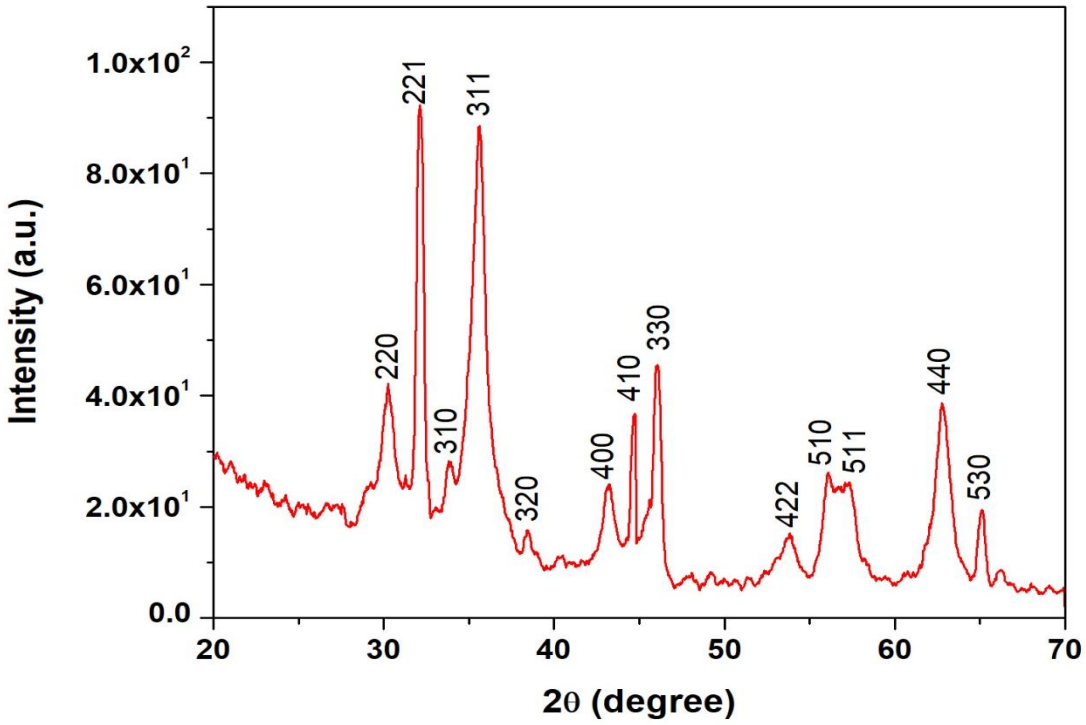

Fig. 23: XRD pattern of iron oxide nanoparticles

Antimicrobial Activity of Iron Oxide Nanoparticles

The antibacterial activity of green synthesized iron oxide NPs using leaf extract of *Coriandrum Sativum* was determined by the agar well diffusion method. From antimicrobial activity evaluation against pathogenic bacteria *Escherichia coli*, it was

found that synthesized iron oxide nanoparticles possess significant antimicrobial properties. The strongest efficiency was obtained at a dose 500 mg/ml of NPs.

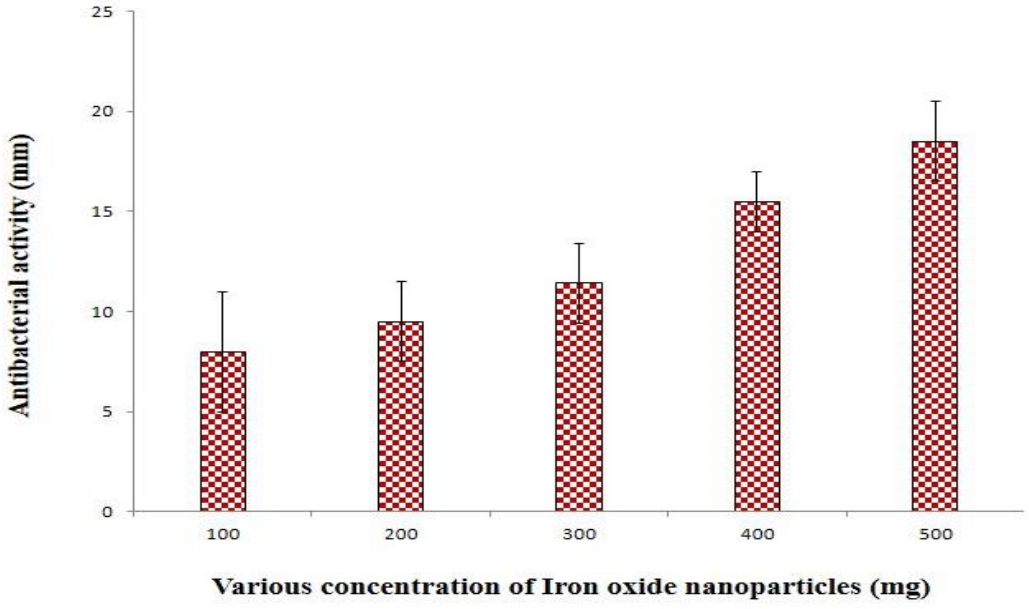

Fig. 24: Antibacterial activity (zone of inhibition, mm) of iron oxide nanoparticles solution against pathogenic *Escherichia coli*.

Chapter 7: General Conclusions

The last chapter 7 deals with general conclusions drawn from the work carried out in the thesis. Key conclusions are outlined as follows:

Present study suggests that the plant-mediated methods of synthesizing metal oxide nanoparticles have proven to be one of the best methods to date. This is due to its cost-effective, simple, efficient and eco-friendly nature.

(1) In present research work, experimental results showed an appreciable reduction in chemical oxygen demand (COD) and chromium (Cr) content of TWW treated with green synthesized TiO_2 NPs during the photocatalytic treatment and thus, convincingly demonstrated the tremendous potential for wastewater treatment and

brings a new direction to the development of nanomaterial-based next-generation wastewater treatment technologies to solve the problem of environmental pollution associated with industrial wastewaters.

(2) Green synthesized copper oxide nanoparticles exhibited as a good anticancer agent when conducted in-vitro cytotoxicological studies on hepatocellular carcinoma HepG2 cancer cell. The results show that the green synthesized copper oxide nanoparticles can be used for the treatment of cancer which is the major threat to modern human society. Green synthesized CuO NPs showed the significant results on the mammalian cell through the killing of cancer cells without any evil effect on hepatocytes. So the CuO NPs synthesized by green chemistry approached, can be successfully applied for the treatment of liver cancer since it has sufficient transport properties and cell membrane penetration power.

(3) FTIR results proved that biomolecules from leaf extract are responsible for bioreduction and the leaf extract act as reducing and capping agents which prevents from the agglomeration of the nanoparticles and thereby stabilizing the nanoparticles.

(4) Present investigation also suggests that the green synthesized zinc oxide nanoparticles and iron oxide nanoparticles exerting an in-vitro toxic effect on human bacterial pathogens Antibacterial studies. The Antimicrobial properties of synthesized nanoparticles were assessed against the bacterial species *Escherichia coli* and were found effective.

References:

[1] M. Batzill, U. Diebold, The surface and materials science of tin oxide, Prog. in Surface Sci. 79 (2005) 47-154.

[2] E.L. Hu, D.T. Shaw, Synthesis and Assembly, Nanostructure Sci Tech, Chapter-2 (1999) 15-33.

[3] N. Kumar, S. Kumbhat, Essentials in nanoscience and nanotechnology, published 2016 by John Wily & Sons, Inc, (2016) 31-74

[4] D. Sharma, S. Kanchi, K. Bisetty, Biogenic synthesis of nanoparticles: A review, Arabian J. of Chem. (2015).

[5] I. Khan, K. Saeed, I. Khan, Nanoparticles: Properties, applications and Toxicities, Arabian J. of Chem. (2017).

[6] S.S. Shankar, A. Ahmd, R. Pasricha, M.J. Sastry, Bioreduction of chloroaurate ions by geranium leaves and its endophytic fungus yields gold nanoparticles of different shapes, Mater Chem. 13 (2003) 1822-1846.

[7] M. D. Carvalho, F. Henriques, L.P. Ferreira, M. Godinho, M. M. Cruz, Iron oxide nanoparticles: the Influence of synthesis method and size on composition and magnetic properties, J. of Solid State Chem. 201 (2013) 144-152.

[8] P. Periyathambi, W. S. Vedakumari, S. Bojja, S. B. Kumar, T. P. Sastry, Green biosynthesis and characterization of fibrin functionalized iron oxide nanoparticles with MRI sensitivity and increased cellular internalization, Mat. Chem. and Phy. 148 (2014) 1212-1220.

[9] M. Behera, G. Giri, Inquiring the photo-catalytic activity of cuprous oxide nanoparticles synthesized by a green route on methylene blue dye, Int. J. Ind. Chem. 7 (2016) 157-166.

[10] A.K. Biswas, Md. R. Islam, Z.S. Choudhury, A. Mostafa, M.F. Kadir, Nanotechnology based approaches in cancer therapeutics, Adv. Nat. Sci.: Nanosci. Nanotechnol. 5 (2014) 043001.

[11] C. Buzea, I. Ivan, B. Pacheco, R. Kevin, Nanomaterials and nanoparticles: Sources and toxicity, Biointerphases. 2 (2007) MR17-MR71.

[12] M.J. Akhtar, M. Ahamed, S. Kumar , M.M. Khan, J. Ahmad, S.A. Alrokayan, Zinc oxide nanoparticles selectively induce apoptosis in human cancer cells through reactive oxygen species, Int. J. Nanomed. 7 (2012) 845-57.

[13] V. Madhubala, T. Kalaivani, Phyto and hydrothermal synthesis of Fe_3O_4@ZnO core-shell nanoparticles using Azadirachta indica and its cytotoxicity studies, App. Surface Sci. 449 (2018) 584-590.

[14] B. Das, S.K. Dash, D. Mandal, T. Ghosh, S. Chattopadhyay, S. Tripathy, S. Das, S.K. Dey, D. Das, Somenath Roy, Green synthesized silver nanoparticles destroy multidrug resistant bacteria via reactive oxygen species mediated membrane damage, Arabian J. of Chem. 10 (2017) 862-876.

[15] F. Davar, A. Majedi, A. Mirzaei, Green Synthesis of ZnO nanoparticles and its application in the degradation of some dyes, J. Am. Ceram. Soc. 98 (2015) 1739-1746.

[16] C.P. Devatha, A. K. Thalla, S.Y. Katte, Green synthesis of iron nanoparticles using different leaf extracts for treatment of domestic waste water, J. of Cleaner Prod. 139 (2016) 1425-1435.

[17] R. Dobrucka, J. Dugaszewska, Biosynthesis and antibacterial activity of ZnO nanoparticles using Trifolium pratense flower extract, Saudi J. of Bio. Sci. 23 (2016) 517-523.

[18] Y.E.K. Hala, M.A. Aly-Eldeen, S.M. Gharib, Green synthesis of iron oxide (Fe_3O_4) nanoparticles using two selected brown seaweeds: Characterization and application for lead bioremediation, Acta Oceanol. Sin. 35 (2016) 89-98.

[19] F.J. Heiligtag, M. Niederberger, The fascinating world of nanoparticle research, Mat. Today. 16 (2013) 262-271.

[120] N.I. Hulkoti, T.C. Taranath, Biosynthesis of nanoparticles using microbes-A review, Colloids and Surfaces B: Biointerfaces. 121 (2014) 474-483.

[121] I. Khan, K. Saeed, I. Khan, Nanoparticles: Properties, applications and toxicities, Arabian J. of Chem. (2017).

[22] S. Lata, S.R. Samadder, Removal of arsenic from water using nano adsorbents and challenges: A review, J. of Env. Mana. 166 (2016) 387-406.

[23] M. Mahdavi, F. Namvar, M.B. Ahmad, R. Mohamad, Green biosynthesis and characterization of magnetic iron oxide (Fe_3O_4) Nanoparticles Using Seaweed (Sargassum muticum) Aqueous Extract, Molecules. 18 (2013) 5954-5964.

[24] N. Matinise, X.G. Fukua, K. Kaviyarasua, N. Mayedwaa, M. Maaza, ZnO nanoparticles via Moringa oleifera green synthesis: Physical properties & mechanism of formation, App. Surface Sci. 406 (2017) 339-347.

[25] C. Mystrioti, T.D. Xanthopoulou, N. Papassiopi, A. Xenidis, Comparative evaluation of five plant extracts and juices for nanoiron synthesis and application for hexavalent chromium reduction, Sci. of the Total Env. 539 (2016) 105-113.

[26] J. Peternela, M.F. Silva, M.F. Vieir, R. Bergamasco, A.M.S. Vieira, Synthesis and Impregnation of Copper Oxide Nanoparticles on Activated Carbon through Green Synthesis for Water Pollutant Removal, Mat. Res. 21 (2016) e20160460.

[27] M. Guzman, J. Dille, S. Godet, Synthesis and antibacterial activity of silver nanoparticles against gram-positive and gram-negative bacteria, Nanomedicine: Nanotechnol., Bio., and Med. 8 (2012) 37-45.

[28] M. Al-Qahtani Khairia, Cadmium removal from aqueous solution by green synthesis zero valent silver nanoparticles with Benjamina leaves extract, Egyptian J. of Aquatic Res. 43 (2017) 269-274.

[29] J. Santhoshkumar, S.V. Kumar, S. Rajeshkumar, Synthesis of zinc oxide nanoparticles using plant leaf extract against urinary tract infection pathogen, Resource-Efficient Technol. 3 (2017) 459-465.

[30] T. Sinha, M. Ahmaruzzaman, Biogenic synthesis of Cu nanoparticles and its degradation behavior for methyl red, Mat. Lett. (2015).

[31] J. Suarez-Cerda, G. Alonso-Nunez, H. Espinoza-Gomez, L.Z. Flores-Lopez, Synthesis, kinetics and photo catalytic study of “ultra-small” Ag-NPs obtained by a green chemistry method using an extract of Rosa 'Andeli' double delight petals, Journal of Colloid and Int. Sci. 458 (2015) 169-177.

[32] A. Gangula, R. Podila, M. Ramakrishna, L. Karanam, C. Janardhana, A.M. Rao, Catalytic Reduction of 4-Nitrophenol using Biogenic Gold and Silver

Nanoparticles Derived from Breynia rhamnoides, Langmuir. 27(2011)15268-15274

[33] P. Banerjee, S. Sau, P. Das, A. Mukhopadhyay, Green synthesis of silver - nanocomposite for treatment of textile dye, Nanosci. Technol. 1(2) (2014) 1-6.

[34] M. Vinothkannan, C. Karthikeyan, G.G. Kumar, A.R. Kim, D.J. Yoo, One-pot green synthesis of reduced graphene oxide (RGO)/Fe_3O_4 nanocomposites and its catalytic activity toward methylene blue dye degradation, Spectrochimica Acta Part A: Molecular and Bio. Spec. 136(2015) 256-264.

[35] Z.Y. Ozkan, M. Cakirgoz, E.S. Kaymak, E. Erdim, Rapid decolorization of Textile wastewater by green synthesized iron nanoparticles, Water Sci. echnol. 77 (2) (2017) 511-517.

[36] G. Sharmila, M.F. Fathima, S. Haries, S. Geetha, N.M. Kumar, C. Muthukumaran, Green synthesis, characterizationand antibacterial efficacy of palladium nanoparticles synthesized using Filicium decipiens leaf extract, J. of Molecular Struc. 1138 (2017) 35-40.

[37] H. Huawe, T. Gang, W. Yejing, C. Rui, C. G. Peng, C. Liqun, Z. Hua, Z. Ping, X. Qingyou, In situ green synthesis and characterization of sericin-silver nanoparticle composite with effective antibacterial activity and good biocompatibility, Mat. Sci. and Eng.: C. 80 (2017) 509-516.